

ANALYSIS AND DESIGN OF CONSTANT-FREQUENCY PEAK-CURRENT-CONTROLLED HIGH-POWER-FACTOR BOOST RECTIFIER WITH SLOPE COMPENSATION

Carlos A. Canesin (✉), and Ivo Barbi (♠)

(✉) Paulista State University
UNESP - FEIS - DEE - P.O. box 31
Fax: (55) 187-622125
e-mail: EEL1CAC@inep.ufsc.br
15378-000 - Ilha Solteira (SP) BRAZIL

(♠) Federal University of Santa Catarina
INEP - P.O. Box 5119
FAX: (55) 48-2319770
E-mail: ivo@inep.ufsc.br
88040-970 - Florianópolis (SC) BRAZIL

Abstract - This paper presents the analysis and the design of a peak-current-controlled high-power-factor boost rectifier, with slope compensation, operating at constant frequency.

The input current shaping is achieved, with continuous inductor current mode, with no multiplier to generate a current reference.

The resulting overall circuitry is very simple, in comparison with the average-current-controlled boost rectifier.

Experimental results are presented, taken from a laboratory prototype rated at 370W and operating at 67kHz. The measured power factor was 0.99, with a input current THD equal to 5.6%, for an input voltage THD equal to 2.26%.

1. INTRODUCTION

Engineers involved in the design of high power factor boost rectifier, recognize that the peak-current-controlled technique has several advantages over the average-current-controlled technique [1]. Those advantages are:

- It is sufficient to sense only the switch current. The use of current transformer reduces losses;
- There is no need for a current-error compensator;
- As there is an instantaneous pulse-by-pulse current limit, the reliability is improved and the response speed is increased.

However, similarly to the average-current-controlled technique, a multiplier is needed to provide a current reference generator to achieve input current shaping.

Reference [2] examines a high-power-factor boost rectifier, where the peak switch current is clamped at a constant value during the input voltage line cycle. The variation of the input voltage and three different modes of operation shape the input current so that a relatively low THD is obtained. The main attribute of the mentioned technique is its simplicity. Furthermore, because it utilizes a general purpose dedicated integrated circuit, it is less expensive than the classical solution discussed in reference [1]. It should be noticed that it is not used any multiplier to generate a current reference.

However, a price is paid to get the simplicity of the circuit. The first consequence is the limit in the input voltage range, so that a universal input operation can not be easily

accomplished. The second one is that the current THD is higher than that obtained with the utilization of the technique described in reference [1].

The simplified circuits diagram of the techniques examined in references [1] and [2] are shown in Figures 1.a and 1.b respectively.

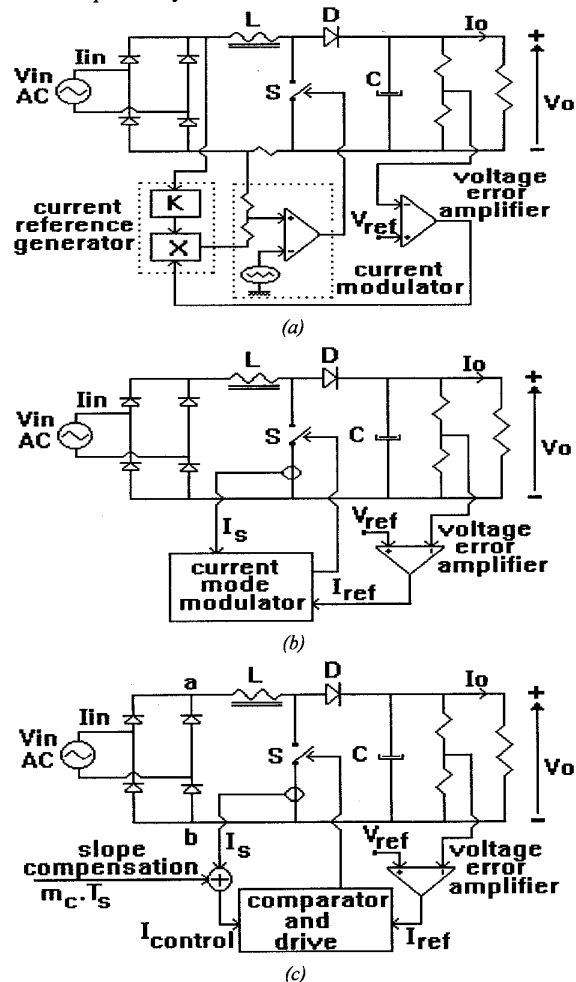


Fig.1 - The boost power-factor correctors with, (a) peak-current control; (b) clamped-current control, and (c) peak-current control with slope compensation.

(✉)C.A.Canesin would like to thank to UNESP-FEIS, UFSC-INEP, and CAPES-PICD, for supporting his Ph.D. studies.

The technique studied in this paper is schematically represented in Figure 1.c. It has been derived from that shown in Figure 1.b, having as the main difference, the inclusion of the slope compensation, allowing the duty-cycle to be larger than 0.5. As it will be demonstrated hereafter, the slope compensation, besides ensuring the needed stability, has strong influence in the power factor and in the THD at the input current. It should be mentioned that the slope compensation was also used in reference [3]. However, the purpose was to provide stability, not to improve the power factor.

The purpose of this paper is to report on the theoretical and experimental studies concerning this method, emphasizing design aspects. It is shown that this technique in this paper referred to a constant-frequency peak-current controlled high-power-factor boost rectifier with slope compensation, is capable of drawing a line current with a THD as small as that obtained with the average-current-controlled boost rectifier.

2. ANALYSIS OF OPERATION

To simplify the analysis, it is assumed that:

- all components are ideal;
- the converter is operating in steady-state at a fixed switching frequency (f_s);
- the f_s is much higher than the AC line frequency (f_{line});
- the input voltage (V_{in}) is a sine-wave;
- the output voltage (V_o) is constant;
- the peak-current reference (I_{ref}) is constant during one period of the AC line. Thus,

$$V_{in}(wt) = V_p \sin(wt) \quad (1)$$

Where: V_p = peak input voltage;

$$w = 2\pi f_{line}$$

With the considerations listed above, the DC voltage V_{ab} is a full-wave rectified sine-wave. Hence,

$$V_{ab}(wt) = V_p |\sin(wt)| \quad (2)$$

In order to explain the operation of the peak-current control, the switch (S) of the Boost converter shown in Figure 1.c is turned on at the beginning of the switching period (T_s) and turned off when the control current ($I_{control}$) reaches the reference current (I_{ref}).

Thus,

$$I_{control}(wt) = I_s(wt) + m_c T_s \quad (3)$$

Where:

$I_s(wt)$ = switch current;

m_c = slope current control;

$$T_s = 1/f_s \quad (4)$$

The boost converter during one period of the voltage V_{ab} can operate in discontinuous or continuous conduction modes. These modes are dependent on V_{ab} , I_{ref} and m_c . For a fixed slope current control and peak-current reference control, it depends only on the voltage V_{ab} .

The DC boundary voltage (V_{abL}) of discontinuous and continuous conduction modes is given by equation (5).

$$V_{abL} = V_o \left[\left(\frac{1-K_r}{2} \right) + \sqrt{\left(\frac{1+K_r}{2} \right)^2 - \frac{K_r I_{ref}}{m_c T_s}} \right] \quad (5)$$

Where: K_r = constant of slope current;

L = inductance of the boost inductor.

$$m_c = K_r \frac{V_o}{L} \quad (6)$$

Therefore, if $V_{ab}(wt)$ is below V_{abL} , the converter operates in discontinuous conduction mode, and above V_{abL} in continuous conduction mode.

In order to stabilize the current loop at the worst operating point, and to provide a minimum harmonic distortion in the input current waveform (I_{in}), the following inequalities should be satisfied.

$$I_{ref\ max} \leq \frac{K_r V_o T_s}{L} \quad (7)$$

and,

$$K_r > 1/2 \quad (8)$$

Where: $I_{ref\ max}$ = maximum value of peak-current reference.

The boundary angle (wt_L) of discontinuous and continuous conduction modes is given by equation (9).

$$wt_L = a \sin \frac{V_{abL}}{V_p} \quad (9)$$

We have the following parameters for normalizing the expressions obtained by analysis:

$$\alpha = \frac{V_o}{V_p} \quad (10)$$

$$V_b = V_o \quad (11)$$

$$I_b = \frac{V_o T_s}{2 L} \quad (12)$$

Where: V_b = base voltage;

I_b = base current.

The normalized peak-current reference ($\overline{I_{ref}}$) is given by equation (13).

$$\overline{I_{ref}} = \frac{I_{ref}}{I_b} = \frac{I_{ref}}{V_o} \frac{2L}{T_s} \quad (13)$$

2.1. DISCONTINUOUS CONDUCTION MODE-DCM

In discontinuous conduction mode the switch duty-cycle is governed by equation (14).

$$D_{dcm}(wt) = \frac{I_{ref}}{(V_{ab}/L + m_c) T_s} \quad (14)$$

Thus, the maximum value of the duty-cycle (δ) in DCM is given as follows:

$$\delta = \frac{I_{ref} \max L}{K_r V_o T_s} \leq 1 \quad (15)$$

It should be pointed out, however, that the value of δ is limited by the PWM-IC and the oscillator timing parameters [4]. Thus,

$$K_r = \frac{I_{ref} \max}{2\delta} \quad (16)$$

Where:

$I_{ref} \max$ = maximum normalized value of the peak-current reference.

Figure 2.a shows the current waveform through the boost inductor in DCM for a generic switching period, where:

$I_{Ldcm}(wt)$ = average instantaneous current through L in DCM.

$$\text{and, } d(wt) = D_{dcm}(wt) \frac{V_{ab}}{V_o - V_{ab}} \quad (17)$$

The normalized average instantaneous current ($\overline{I_{Ldcm}(wt)}$) through the boost inductor in DCM, and normalized boundary angle (\overline{wt}_L), are given by equations (18) and (19) respectively.

$$\overline{I_{Ldcm}(wt)} = \frac{\overline{I_{ref}^2} |\sin(wt)|}{\left\{ A \overline{I_{ref}^2} + B |\sin(wt)| + C |\sin(wt)|^2 - D |\sin(wt)|^3 \right\}} \quad (18)$$

$$\text{Where: } A = \frac{\alpha}{\delta^2}; \quad B = \frac{\overline{I_{ref}}(4\delta - \overline{I_{ref}})}{\delta};$$

$$C = \frac{4(\delta - \overline{I_{ref}})}{\alpha \delta}; \quad D = \left(\frac{2}{\alpha}\right)^2$$

$$\overline{wt}_L = a \sin \left\{ \alpha \left[\left(\frac{2\delta - \overline{I_{ref}}}{4\delta} \right) + \sqrt{\left(\frac{2\delta + \overline{I_{ref}}}{4\delta} \right)^2 - \frac{\overline{I_{ref}}}{2}} \right] \right\} \quad (19)$$

2.2. CONTINUOUS CONDUCTION MODE-CCM

In continuous conduction mode the switch duty-cycle is given by equation (20).

$$D(wt) = 1 - \frac{V_p |\sin(wt)|}{V_o} \quad (20)$$

The current waveform through L in CCM for a generic switching period is shown in Figure 2.b, where:

$I_L(wt)$ = average instantaneous current through L in CCM.

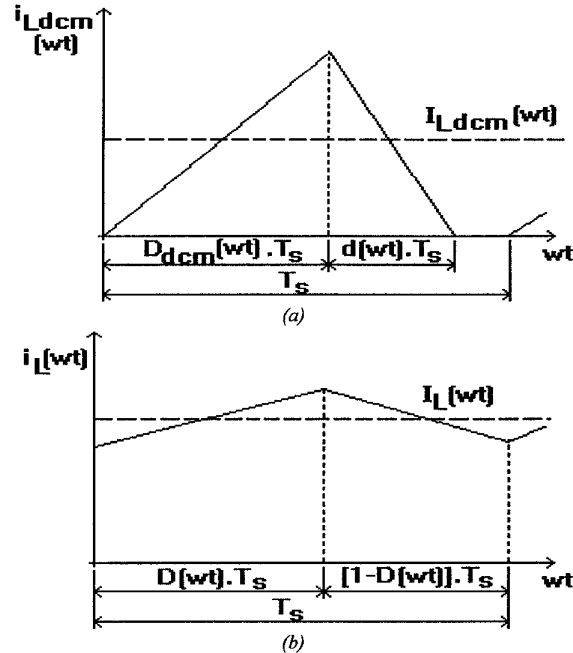


Fig.2 - Current through L in: (a) DCM; (b) CCM.

Equation (21) governs the normalized average instantaneous current ($\overline{I_L(wt)}$) through L in CCM.

$$\overline{I_L(wt)} = \overline{I_{ref}} - \frac{\overline{I_{ref}}}{\delta} + \frac{(\overline{I_{ref}} - \delta) \sin(wt)}{\alpha \delta} + \frac{|\sin(wt)|^2}{\alpha^2} \quad (21)$$

2.3. NORMALIZED AVERAGE LOAD CURRENT AND THE NORMALIZED CONTROL LAW

The normalized average instantaneous current ($\overline{i_L(wt)}$) through L over the period of V_{ab} is given by equation (22).

$$\overline{i_L(wt)} = \begin{cases} \overline{I_{Ldcm}(wt)} & \text{if: } \begin{cases} 0 \leq wt < wt_L \\ \pi - wt_L < wt \leq \pi \end{cases} \\ \overline{I_L(wt)} & \text{if: } wt_L \leq wt \leq \pi - wt_L \end{cases} \quad (22)$$

The normalized average current ($\overline{I_{Lav}}$) through L for a line period is given by equation (23).

$$\overline{I_{Lav}} = \frac{1}{\pi} \left\{ \int_0^{wt_L} \overline{I_{Ldcm}(wt)} dt + \int_{wt_L}^{\pi - wt_L} \overline{I_L(wt)} dt + \int_{\pi - wt_L}^{\pi} \overline{I_{Ldcm}(wt)} dt \right\} \quad (23)$$

Thus, the normalized average load current ($\overline{I_o}$) is still governed by expression (24).

$$\overline{I_o} = \left(\frac{2}{\pi \alpha} \right) \overline{I_{Lav}} \quad (24)$$

Figure 3 shows the normalized control law obtained by equation (24).

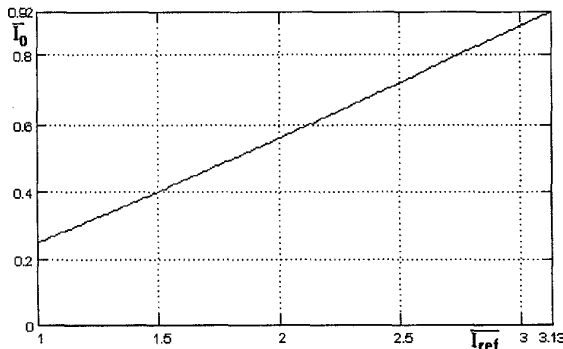


Fig.3 - Normalized control law for $\alpha = 1.0932$ and $\delta = 0.94$.

Figure 4 shows the normalized input current ($\overline{I_{in}(wt)}$) as function of the normalized peak-current reference, governed by equation (25).

$$\overline{I_{in}(wt)} = \begin{cases} \overline{i_L(wt)} & \text{if: } 0 \leq wt \leq \pi \\ -\overline{i_L(wt)} & \text{if: } \pi < wt \leq 2\pi \end{cases} \quad (25)$$

3. DESIGN OF THE BOOST INDUCTANCE (L) AND THE CONSTANT OF SLOPE CURRENT (K_r)

The normalized ripple current through L in continuous conduction mode is governed by equation (26) and it is shown in Figure 5.

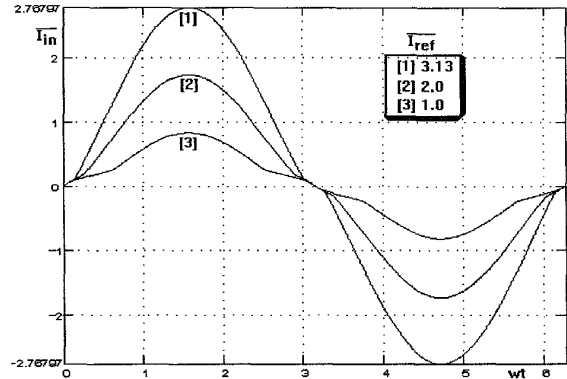


Fig.4 - Normalized input current for $\alpha = 1.0932$ and $\delta = 0.94$.

$$\overline{\Delta I_L(wt)} = |\sin(wt)| - \frac{|\sin(wt)|^2}{\alpha} \quad (26)$$

Therefore, the inductance L is given by equation (27).

$$L = \frac{V_p T_s \overline{\Delta I_{Lmax}}}{\Delta I_{Lmax}} \quad (27)$$

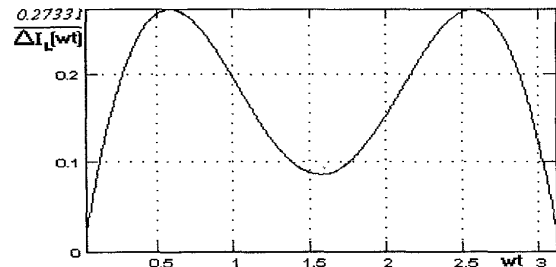


Fig. 5 - Normalized ripple current through L for $\alpha = 1.0932$.

It is assumed that:

$$\Delta I_{Lmax} = 0.2 I_{inp} \quad (28)$$

$$I_{inp} = \frac{\sqrt{2} P_o}{\eta V_{in(rms)min}} \quad (29)$$

Where:

P_o = nominal output power ;

η = minimum efficiency assumed ;

$V_{in(rms)min}$ = minimum rms input voltage.

From equation (15), the constant of slope current (K_r) is governed by following equation.

$$K_r = \frac{I_{refmax} L}{V_o T_s \delta} \quad (30)$$

With, $I_{refmax} = I_{inp} + m_c D_{min} T_s \quad (31)$

Where: $D_{min} = (\alpha - 1)/\alpha \quad (32)$

$$\text{Thus, } K_r = \frac{I_{inp} L}{V_p T_s (1 - \alpha + \alpha \delta)} \quad (33)$$

Therefore, with the input and output data of the boost converter it is possible to select the inductance value of the boost inductor from equation (27), the constant of slope current value from equation (33), and from equation (16) the maximum value of normalized peak-current reference corresponding to the nominal output power.

4. POWER FACTOR AND THE TOTAL HARMONIC DISTORTION

The normalized power factor is governed by equation (34) and it is shown in Figure 6.a, as function of the normalized peak-current reference.

$$\overline{PF} = \frac{\overline{P_{in}}}{\overline{V_{in(rms)}} \overline{I_{in(rms)}}} \quad (34)$$

With,

$$\overline{P_{in}} = \frac{1}{\pi \alpha} \int_0^{\pi} |\sin(\omega t)| |i_L(\omega t)| d\omega t \quad (35)$$

$$\overline{I_{in(rms)}} = \sqrt{\frac{1}{\pi} \int_0^{\pi} [i_L(\omega t)]^2 d\omega t} \quad (36)$$

$$\overline{V_{in(rms)}} = \frac{1}{\alpha} \sqrt{\frac{1}{\pi} \int_0^{\pi} |\sin(\omega t)|^2 d\omega t} \quad (37)$$

Where:

$\overline{P_{in}}$ = normalized input power ;

$\overline{V_{in(rms)}}$ = normalized input rms voltage ;

$\overline{I_{in(rms)}}$ = normalized input rms current.

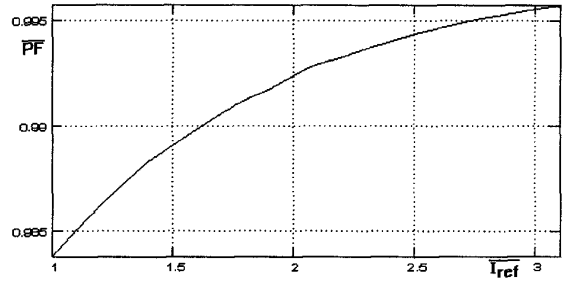
The normalized total harmonic distortion is given by equation (38) and it is shown in Figure 6.b, as function of the normalized peak-current reference.

$$\overline{THD} = \sqrt{\left(\frac{\cos \phi}{\overline{PF}}\right)^2 - 1} \quad (38)$$

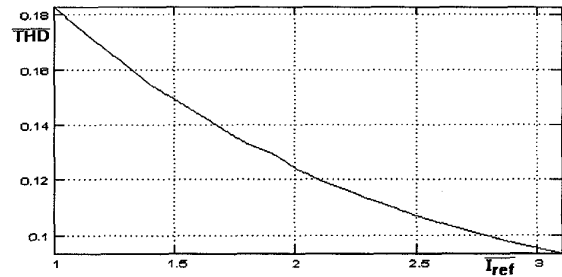
Where we suppose that the displacement angle is zero. Thus,

$$\cos \phi = 1 \quad (39)$$

The normalized harmonic rms input current ($\overline{I_{in(rms),n}}$) content in relation to the fundamental rms input current ($\overline{I_{in(rms),1}}$) are shown in Figure 7 as function of the normalized peak-current reference.



(a)



(b)

Fig. 6 - (a) Normalized power factor, and (b) Normalized total harmonic distortion, for $\alpha = 1.0932$ and $\delta = 0.94$.

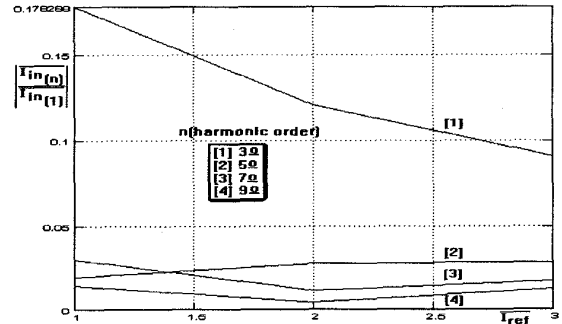


Fig. 7- Normalized rms input current harmonic for $\alpha = 1.0932$ and $\delta = 0.94$.

Figure 8 shows the normalized harmonic rms input current content in relation to the normalized fundamental rms input current, taking as example: $\alpha = 1.0932$, $\delta = 0.94$ and $\overline{I_{ref}} = 3.13$.

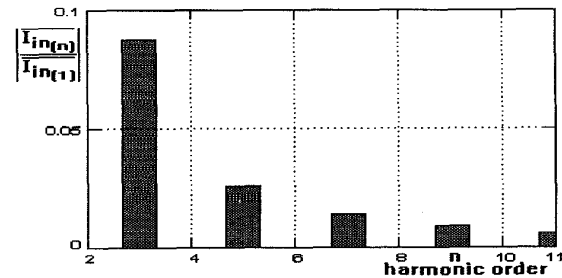


Fig. 8- Normalized rms current harmonic contents for $\alpha = 1.0932$,

$\delta = 0.94$ and $\overline{I_{ref}} = 3.13$.

5. DESIGN PROCEDURE AND EXAMPLE

The design procedure and example of the proposed clamped-current boost rectifier with slope compensation is described as follows:

■ Step 1- Input and output data specifications.

$V_p = 311V$; $f_{line} = 60Hz$; $V_{in(rms)min} = 187V$; $V_o = 340V$
 $P_o = 374W$; $\eta = 0.95$; $f_s = 67kHz$; and $\delta = 0.94$.

■ Step 2- Maximum normalized ripple value of the current through L ($\overline{\Delta I_{Lmax}}$).

The parameter (α) is governed by equation (10). So, from input and output data we can obtain:

$$\alpha = V_o / V_p = 1.0932.$$

Known (α) and from equation (26), the maximum normalized ripple value ($\overline{\Delta I_{Lmax}}$) can be obtained. From Figure 5 for $\alpha = 1.0932$, one obtain:

$$\overline{\Delta I_{Lmax}} = 0.273.$$

■ Step 3- Calculation of the boost inductance value (L).

The peak input current value (I_{inp}) is given by equation (29). From parameters specified in Step 1, we obtain:

$$I_{inp} = 2.98A.$$

Furthermore, the maximum ripple value of the current through L (ΔI_{Lmax}) is given by equation (28). Thus,

$$\Delta I_{Lmax} = 0.596A.$$

Therefore, with the parameters specified in Step 1, known ($\overline{\Delta I_{Lmax}}$), and (ΔI_{Lmax}), the inductance L can be obtained from equation (27). Thus,

$$L = 2.13mH.$$

■ Step 4- Constant of slope current value (K_r).

With the parameters shown in Step 1, known (α), (I_{inp}), and (L), the constant of slope current value (K_r) is given by equation (33). Thus,

$$K_r = 1.5.$$

■ Step 5- Nominal normalized average load current value ($\overline{I_{onom}}$).

With the parameters shown in Step 1, the nominal average load current value (I_{onom}) is given by equation (40).

$$I_{onom} = P_o / V_o \quad (40)$$

The nominal normalized average load current value ($\overline{I_{onom}}$) is given by equation (41).

$$\overline{I_{onom}} = I_{onom} / I_b \quad (41)$$

Where:

$$I_b = \frac{V_o T_s}{2L} = 1.1912A.$$

Thus,

$$\overline{I_{onom}} = 0.92.$$

■ Step 6- Maximum normalized value of the peak-current reference ($\overline{I_{refmax}}$).

From equations (23) and (24), known (α), and (δ), the normalized control law can be obtained by equation (24). So, from Figure 3 and known (α), and (δ), we can obtain the

($\overline{I_{refmax}}$) value to the ($\overline{I_{onom}}$) value. Thus,

$$\overline{I_{refmax}} = 3.13.$$

■ Step 7- Capacitance of the output filter value (C).

The capacitance (C) required to achieve the output ripple voltage (ΔV_o) specification less than 5%, is given by equation (42).

$$C \geq \frac{P_o}{2\pi \cdot 120 \cdot V_o \cdot \Delta V_o} \quad (42)$$

So, it is assumed that: $C = 100\mu F$.

Figure 9 shows the input current and voltage waveforms, which have been generated by simulation for the design example.

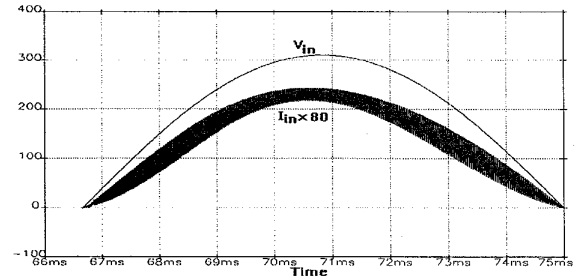


Fig. 9- Simulation input current and voltage.

6. EXPERIMENTAL RESULTS

The specified components and the values of the parameters for the implemented circuit from the design example, shown in Figure 10, are the following :

- switch S: APT5040; - diode D: MUR850;
- PWM-I.C.: UC3842;
- input filter inductor L : 2.13mH (core E42/20);
- output filter capacitor C : 100 μF / 500V ;
- input diodes: 4 x 1N5404.

The experimental input current and voltage are shown in Figure 11 at full load and half load.

The experimentally obtained waveforms shown in Figure 11 are in agreement with the results predicted theoretically. It should be pointed out, however, that the voltage drop at the input rectifier diodes have not been considered in the analysis.

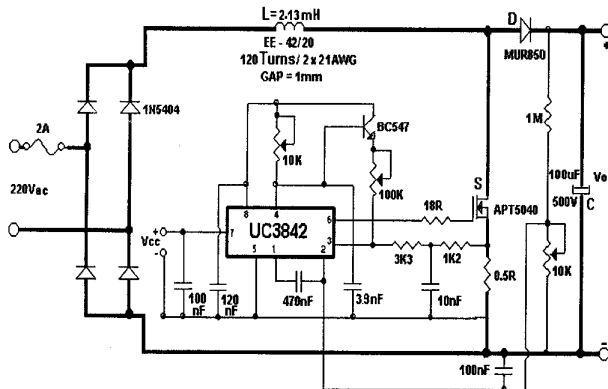


Fig.10- Implemented current-controlled high-power factor Boost converter circuit.

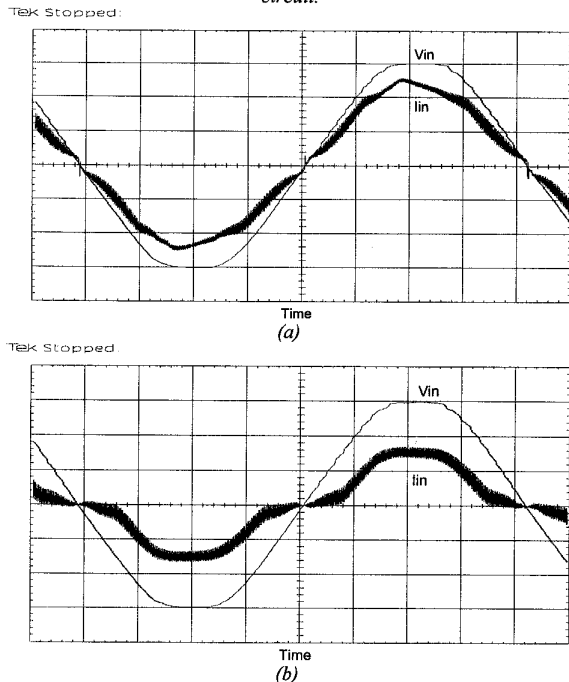


Fig.11 - Experimental input current and voltage at: (a) full load, and (b) half load.
voltage: 100V/div; current: 1A/div
time scale: 2ms/div

The experimental results shown in Figure 11 demonstrate that by adding a ideal slope compensation, a high-power-factor is achieved for a wide load at constant frequency, and the total harmonic distortion at full load is very low.

The experimental results are obtained with the TDS520 Oscilloscope and analyzed by a Fast Fourier Transform algorithm (FFT).

Figure 12.a shows the experimental power factor, and Figure 12.b shows the experimental input current THD, as function of the output current. This result demonstrates that the power-factor is practically near of the unity (0.99) for full load, and the input current THD is equal to 5.6%, for an input voltage THD equal to 2.26%.

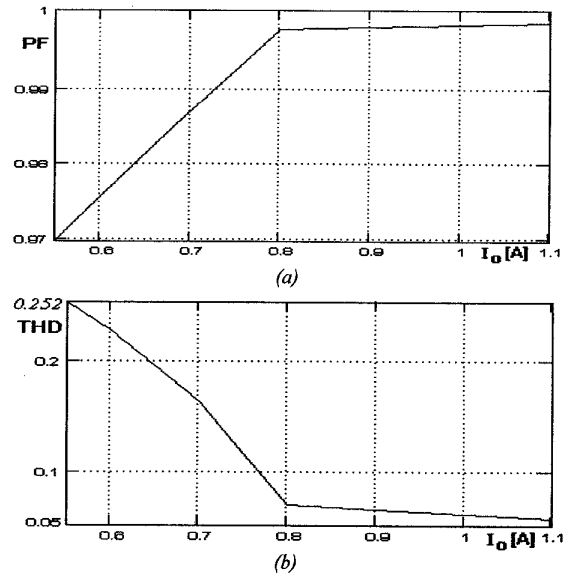


Fig.12 -(a) Experimental power factor; (b) Experimental input current THD.

6. CONCLUSION

From the theoretical and experimental studies described in this paper, concerning with a clamped-current boost rectifier with slope compensation, we can draw the conclusions as follows:

- High-power factor is achieved through slope compensation for a wide load and wide input voltage range;
- The total harmonic distortion of the input current is very low;
- The system stability is inherent for the control technique used, with a fast dynamic response;
- A simple circuitry is the greatest advantage of this technique, in comparison with the average current control;
- This technique presents intrinsic continuous protection of the currents through the switches;
- An inherent overload protection, without necessity of the soft-start and overload current protection circuits is achieved.

Therefore, this technique offers advantages in power-factor correction applications, in comparison with the average current control technique.

REFERENCES

- [1] R. Redl, and B. P. Erisman, "Reducing distortion in peak-current-controlled boost power-factor correctors", *IEEE APEC RECORDS*, pp.576-583, 1994;
- [2] D. Maksimovic, "Design of the clamped-current high-power-factor boost rectifier", *IEEE APEC RECORDS*, pp.584-590, 1994;
- [3] J. Spangler, B. Hussain, and A. K. Behera, "Electronic Fluorescent Ballast using a power factor correction techniques for loads greater than 300Watts", *IEEE APEC RECORDS*, pp.393-399, 1991;
- [4] Unitrode Corporation, "Application Notes U-97 , U-100, and U-101", *Application Notes-Unitrode-USA*, 1986.